Proceedings of Meetings on Acoustics

Volume 9, 2010 http://asa.aip.org

159th Meeting
Acoustical Society of America/NOISE-CON 2010
Baltimore, Maryland
19 - 23 April 2010
Session 4aSA: Structural Acoustics and Vibration

4aSA10. On the use of energy based metrics in active structural acoustic control

Daniel A. Manwill*, Jeff M. Fisher, Scott D. Sommerfeldt, Kent L. Gee and Jonathan D. Blotter

***Corresponding author's address: Mechanical Engineering, Brigham Young University, Brigham Young University, Provo, UT 84602, dmanwill@gmail.com**

Given the benefits of using acoustic energy density for active noise control in enclosures, it was hypothesized that active structural acoustic control (ASAC) might also benefit by incorporating an energy-based structural error quantity. Power flow, or structural intensity, and structural energy density were studied for use in an ASAC system. Power flow was found to be unsuitable for general-purpose use in this application. Its minimization properties are such that for a general case, it may be impossible to predict structural or acoustic response based on a minimization of power flow amplitude in a two-dimensional setting. Additionally, sensor placement is complicated by the large changes in power flow field orientation caused by a small mass loading for a lightweight structure. Structural energy density was found to be a suitable error metric, and provides a slight improvement over velocity-based ASAC in enclosed spaces. A genetic algorithm was used to study structural energy density sensor placement on a simply supported plate. At modal frequencies, optimum control was achieved by placing the sensor at antinodes. The placement of the control force was found to be less critical, but showed a slight tendency towards locations remote from the disturbance force with low velocity cross-derivative.

Published by the Acoustical Society of America through the American Institute of Physics

 [DOI: 10.1121/1.3489240]
Received 14 Aug 2010; published 25 Aug 2010

INTRODUCTION

This paper was originally to have been titled *Real-Time Active Control of Structural Energy Density and Structural Power Flow*, however, the title was changed to more accurately reflect the final scope of the work performed. Additionally, as the construction of the physical real-time control system described in the original abstract was being finalized, some numerical results were produced which led to a suspension of the experimental work described in the original abstract. The revised abstract summarizes the numerical results and indicates the weaknesses of the originally proposed methods.

Active noise control (ANC) has been used as a technique for reduction of unwanted noise in locations such as vehicle cabins where the addition of massive damping materials is impractical. Control is achieved by measuring and minimizing some acoustic quantity at discrete locations in the region of interest. These sensor locations must be chosen carefully such that the acoustic quantity of interest can be easily detected and is also correlated with the global acoustic response. Acoustic energy density based control, which minimizes both potential and kinetic energy in the acoustic field, has been shown to provide good active noise control performance with decreased sensitivity to sensor placement[1].

Active Structural Acoustic Control (ASAC) has also been proposed as a noise mitigation technique for situations where the primary source of unwanted noise is a vibrating structure. Rather than directly controlling some acoustic quantity as occurs in ANC, ASAC involves the control of a structural metric. The metric and minimization location on the structure are chosen such that upon control, the structural radiation is also minimized. Although often difficult to implement, ASAC makes possible a more compact control system that achieves global sound level reductions by eliminating noise at the source. The objective of this research was to determine if an energy-based structural quantity might be incorporated into ASAC such that sensitivity to sensor placement is reduced and performance is improved as happens when acoustic energy density is incorporated into a standard ANC system.

Power Flow

The first quantity considered for use in an ASAC system is power flow, also known as structural intensity. Power flow is a vector quantity describing the linear density of normal energy flux from one region of a structure to another. The basic equations for power flow due to transverse displacements in thin plates were set forth by Noiseaux[2] and are provided in a geometrically descriptive format below. Since energy in a plate is not constrained to flow in only one direction, power flow has both x and y components which are given by equations 1 and 2 respectively.

$$Q_x = \left(\frac{D}{2}\right)\left[\frac{\partial}{\partial x}\left(\frac{\partial^2 W}{\partial y^2}+\frac{\partial^2 W}{\partial x^2}\right)\left(\frac{\partial^* W}{\partial t}\right)-\left(\frac{\partial^2 W}{\partial x^2}+\upsilon\frac{\partial^2 W}{\partial y^2}\right)\left(\frac{\partial^{2*} W}{\partial x \partial t}\right)-(1-\upsilon)\left(\frac{\partial^2 W}{\partial x \partial y}\right)\left(\frac{\partial^{2^*} W}{\partial y \partial t}\right)\right] \quad (1)$$

$$Q_y = \left(\frac{D}{2}\right)\left[\frac{\partial}{\partial y}\left(\frac{\partial^2 W}{\partial y^2}+\frac{\partial^2 W}{\partial x^2}\right)\left(\frac{\partial^* W}{\partial t}\right)-\left(\frac{\partial^2 W}{\partial y^2}+\upsilon\frac{\partial^2 W}{\partial x^2}\right)\left(\frac{\partial^{2*} W}{\partial y \partial t}\right)-(1-\upsilon)\left(\frac{\partial^2 W}{\partial x \partial y}\right)\left(\frac{\partial^{2^*} W}{\partial x \partial t}\right)\right] \quad (2)$$

Physically, each term in the power flow is a product of a generalized force and a generalized velocity. W is the transverse displacement of the plate, x and y are plate dimensions, and D is the bending stiffness of the plate, given below as equation 3, where E is the elastic modulus of the plate, h is thickness, and υ is Poisson's Ratio. The use of an asterisk indicates a complex conjugate.

$$D = \frac{Eh^3}{12\left(1-\nu^2\right)}. \quad (3)$$

The path integral of the normal component of the power flow field around any region gives the net energy flux out of or into that region. The idea behind power flow control is to reduce the amplitude of vibration in a certain

region of a structure by blocking the flux of energy into that region. This approach has been used successfully by Schwenk and Sommerfeldt[3] and Tanaka[4] in the control of beam and plate vibrations respectively.

Power flow has also received some mention in connection with structural radiation. Piaud[5] concluded that for an infinite plate, the power flow and in-plane acoustic intensities were approximately proportional. Mei[6], in a paper primarily concerned with modeling structural response to acoustic and mechanical excitation, mentioned an equivalence between the reactive components of both structural and acoustic intensity fields under control.

Power Flow-Acoustic Relationships

As a precursor to more quantitative analysis of relationships between power flow and the acoustic response that might lead to control implementations, simple experiments were performed in which a steel and aluminum plates were excited mechanically by a shaker and acoustically by a speaker simultaneously at various frequencies. The phase between the two excitations was changed and the power flow field was measured using a Scanning Laser Doppler Vibrometer (SLDV) and finite differencing. **Figure 1** shows a set of power flow maps from one such experiment at 44 Hz. The map on the left was captured with the phase difference between the acoustic and structural excitation set to 60 degrees. The map on the right was captured after the phase was changed to 120 degrees. As can be seen, the source and sink regions have nearly traded places.

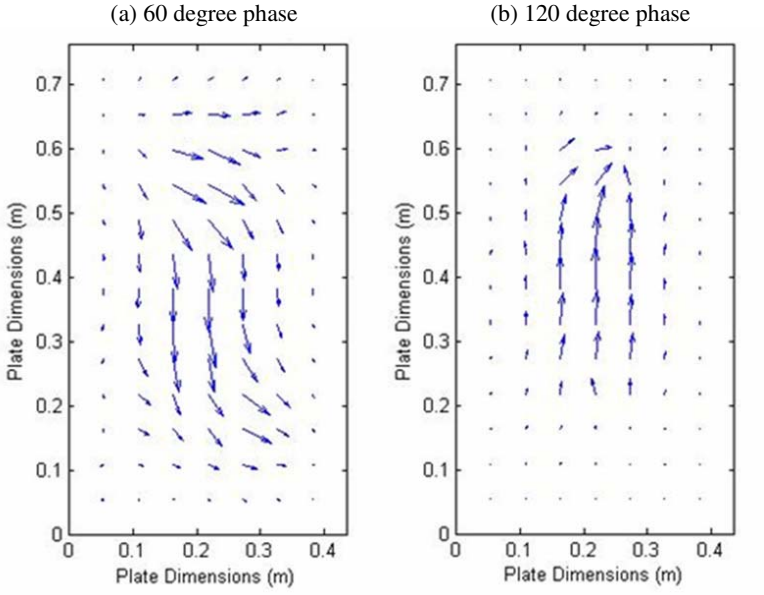

FIGURE 1. Power flow patterns in a clamped steel plate excited simultaneously by an electrodynamic shaker and loudspeaker phased at (a) 60 degrees, (b) 120 degrees

The ability of the acoustic and structural source to interact and cause large changes in the power flow field led to further work to try to clarify these relationships and identify any reciprocities by which the acoustic response might be controlled by means of controlling power flow. A second set of experiments of similar nature involved the measurement or estimation of the acoustic intensity in the near field above the plate as the phase angle between two structural sources was changed. In several cases, behavior was seen which seemed to indicate that regions in the power flow map corresponding to sources or sink were correlated with acoustic sources. Upon further investigation using 3-D quiver plots, the sources and sinks were found to be correlated with circulating near-field energy, rather than energy radiating to the far field.

Controllability of Power Flow

In addition to physical connections between an error metric and the desired control outcome, the incorporation of any quantity into an active control system requires knowledge of how that quantity behaves under minimization. This section describes the controllability and behavior of power flow under minimization.

In their work on progressive waves, Sakano and Tanaka[8] note that there are two methods of reducing power flow. The first is to minimize overall response levels, which is generally beneficial in reducing acoustic radiation. The second is to simply reshape the response to have a purely modal shape, under which conditions power flow is substantially reduced even if vibration amplitude is not. Thus, simple minimization of power flow may not provide predictable results.

Additional difficulty is encountered in sensor placement due to the effect that a small mass loading has on the power flow field. A clamped steel plate excited by two shakers was measured using the SLDV both before and after seven small accelerometers were attached to its surface. The power flow changed substantially, indicating that small mass loadings change a lightweight system sufficiently to make sensor placement an iterative problem in which results may be so sensitive to changes in the system that long-term stability is impossible.

Finally, an effort was made to use optimization to study sensor placement, minimization, and coupling acoustic relationships in an ideal and noiseless mathematical realm. A simply supported steel plate excited by control and disturbance forces was simulated using the modal expansion found in reference 8. Rayleigh's integral was used to estimate the acoustic response. A genetic algorithm was then designed to select structural locations at which minimization of power flow would also result in minimization of acoustic intensity.

These simulations indicated inconsistent and often poor performance. The principal cause of these problems was discovered through analysis of gain-gain-error contour plots, a representative set of which is give in **Figure 2**. Each plot shows contours of power flow magnitude at an error sensor location as the real and imaginary part of the transfer function between disturbance and control forces was varied over the range of +/-4. The figure on the left shows behavior which lends itself to repeatable and predictable control: a single minimum exists, and the contours are shaped such that a least-squares algorithm would easily find the minimum. The figure on the right shows the same contours for the same structure, but at 100 Hz instead of 95 Hz. In this case, the minimum value of power flow does not occur at a single point, but rather corresponds to an entire range of controller gains. The lack of a unique control solution precludes the possibility of deterministically controlling the acoustic response by minimizing power flow amplitude at the numerous frequencies which exhibit this behavior.

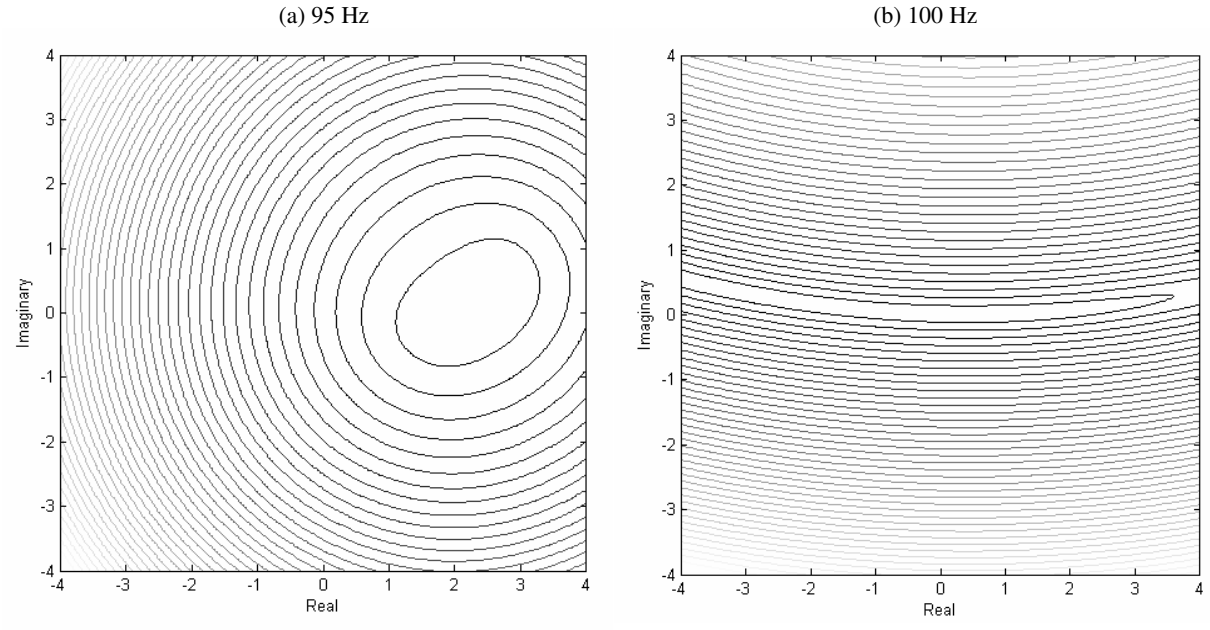

FIGURE 2. Contours of power flow amplitude in a simulated simply supported plate as the real and imaginary components of the control gain are varied between -4 and +4. The plot on the left (a) shows a case for which a single minimum exists. The plot on the right (b) shows a case for which an infinite number of minima exist, making control results unpredictable.

Several underlying principles provide some insight into why minimizing power flow might produce inconsistent results. First, power flow is a gradient quantity. As an analogy, changing the slope of a line does not change the intercept because one degree of freedom remains uncontrolled. Second, power flow is a vector quantity. Since the zero vector can have any direction, minimization of power flow amplitude again leaves a degree of freedom unconstrained.

Structural Energy Density

The second energy-based quantity studied is the structural energy density (SED). SED is less recognized than power flow, but does receive occasional mention in the literature. The basic equation for structural energy density in a plate can be found in Timoshenko[7]. It is given here as equation 4 using the same notation as the power flow equations. An additional variable ρ, the per-area mass of the plate, is included in the last term. The first three terms represent local elastic potential energy storage, while the fourth term represents the local kinetic energy in the plate.

$$SED = \left(\frac{D}{2}\right)\left[\left(\frac{\partial^2 W}{\partial x^2}\right)^2 + \left(\frac{\partial^2 W}{\partial y^2}\right)^2 + 2\upsilon\left(\frac{\partial^2 W}{\partial x^2}\right)\left(\frac{\partial^2 W}{\partial y^2}\right) + 2(1-\upsilon)\left(\frac{\partial^2 W}{\partial x \partial y}\right)^2\right] + \left(\frac{\rho}{2}\right)\left(\frac{\partial W}{\partial t}\right)^2 \quad (4)$$

To the author's knowledge, SED has not as yet been employed directly in any type of active structural or acoustic control. In their paper on progressive wave control of structures, Sakano and Tanaka (8) note that the area integral of the total energy in a plate is minimized upon minimization of progressive waves. No connections are made, however, between this integrated form of SED and the acoustic response, and no effort was made to control SED directly.

Structural Energy Density-Acoustic Relationships

As with power flow, initial experiments in relationships between structural energy density and acoustic intensity showed signs of correlation but did not yield easily extracted relationships that could be applied to the design of a control system. Again, genetic optimization tools were used to extract key behaviors. As these simulations were more successful than in the case of power flow, they are described in greater detail.

The physical basis for the genetic algorithm simulation was a simply supported steel plate radiating into free space. The dimensions of the plate were 508x762x2 mm. An elastic modulus of 210 GPa was used, with Poisson's ratio 0.29, density 7800 kg/m^3, and damping factor 0.001. The response of the plate to a point force was calculated using the modal decomposition employed by Sakano and Tanaka[8]. Rayleigh's integral was used to predict sound pressure at 5, 10, and 15 cm above the plate, and the acoustic intensity was estimated by finite differences.

The fitness function in the genetic algorithm was based on the amplitude of the net radiated intensity of the sound field above the plate. The chromosome was composed of 4 genes, two each corresponding to the x and y positions of the error sensor and control force. As an intermediate step in the evaluation of each chromosome, a shrinking-bound optimization (similar to a bisection method) was used to determine the magnitude and phase to be applied to the control force such that SED at the sensor location was minimized. Designs with better fitness were those that achieved the highest level of minimization in net acoustic intensity upon minimization of structural energy density. As an effort to avoid sensor locations at which structural energy density levels would be in the noise floor of a real physical measurement system, the gain-finding subroutine was limited in magnitude accuracy such that structural energy density could not be minimized to less than 2% of the global uncontrolled maximum value. Finally, due to the long computation times required, only the first 16 structural modal frequencies were studied.

The genetic algorithm showed consistently achievable levels of attenuation at all frequencies. **Table 1** lists the first 16 modes, their corresponding frequencies, and the attenuation achieved at each relative to the uncontrolled level at that frequency. Interestingly enough, 17dB is equal to a 98% reduction, the maximum allowed reduction in structural energy density levels.

TABLE (1). Modes, frequencies, and attenuations in net radiated acoustic intensity achieved under genetically optimized control of structural energy density in a simply supported steel plate.

Mode	Frequency (Hz)	dB Attenuation
(1,1)	27.52	17.01
(1,2)	52.93	17.01
(2,1)	84.68	17.14
(1,3)	95.27	17.14
(2,2)	110.09	17.12
(2,3)	152.43	17.23
(1,4)	154.54	17.00
(3,1)	179.95	17.02
(3,2)	205.35	16.99
(2,4)	211.70	17.12
(1,5)	230.76	17.05
(3,3)	247.69	17.17
(2,5)	287.92	17.12
(3,4)	306.97	17.00
(4,1)	313.32	17.13
(1,6)	323.91	17.12

While attenuation levels were very consistent, sensor placement from one frequency to the next varied quite a bit when viewed from a geometric standpoint. To clarify the critical features of sensor placement, two analyses were undertaken. The first was to normalize position by converting geometric position to nodal positions. A nodal position of 0 corresponds to the sensor being placed at a node, while a nodal position of 1 corresponds to placement at an antinode. The second analysis consisted of determining which of the four terms in structural energy density was being targeted in order to reduce the acoustic response. This involved expressing sensor position by dividing the amplitude of some response metric at the sensor location by an estimate of the global maximum of that metric. The response metrics used were the velocity and three spatial partial derivatives found in the structural energy density expression. Since the velocity and non-mixed second partial derivatives all have the same spatial distribution, it was sufficiently descriptive to study sensor placement as a percentage of maximum velocity and maximum cross derivative. The results of these normalizations are shown in **Table 2**.

TABLE (2). Genetically optimized sensor placement results for 16 modes of a simply supported steel plate. Sensor placement is expressed by nodalized coordinates, which reflect proximity to antinodes, and as velocities and cross derivative at the sensor location as a percentage of global maximum values.

Mode	Nodalized X	Nodalized Y	Velocity Percentage	d^2W/dxy Percentage
(1,1)	0.996	0.994	100	0
(1,2)	0.993	0.992	100	0
(2,1)	0.997	0.979	102	0
(1,3)	0.984	0.970	101	0
(2,2)	0.980	0.982	102	0
(2,3)	0.976	0.987	103	1
(1,4)	0.991	0.990	100	0
(3,1)	0.982	0.977	100	0
(3,2)	0.975	0.981	100	0
(2,4)	0.977	0.986	102	0
(1,5)	0.978	0.941	100	0
(3,3)	0.959	0.961	101	0
(2,5)	0.993	0.974	102	0
(3,4)	0.966	0.986	100	0
(4,1)	0.986	0.983	102	0
(1,6)	0.966	0.989	101	0

As shown, sensor placement was consistently very near antinodes, and at locations of maximum velocity and minimum cross-derivative. In essence, control of the acoustic response is achieved by minimization of structural velocity and non-mixed second order spatial derivatives. Note that percentages greater than 100 indicate that the

sensor was genetically placed at a location with higher velocity than was found at any location on the grid of points used to estimate the maximum velocity.

Information about secondary control force actuator placement is much less consistent than that of sensor placement, and is better represented with histograms rather than tables. The strong antinode-seeking behavior of the sensor was not replicated, but some general trends can be seen in the histograms of **Figure 3**.

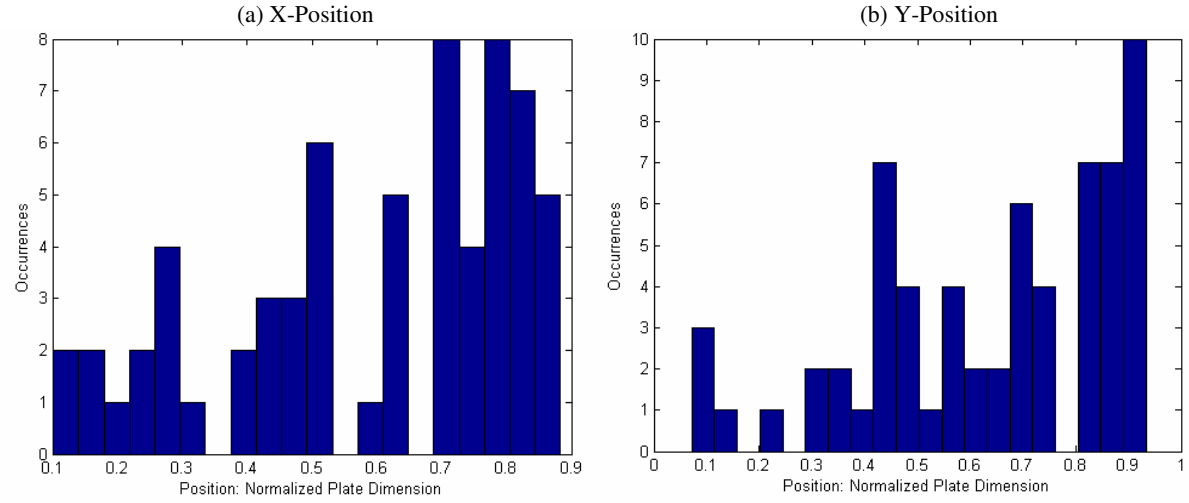

FIGURE 3. Genetically optimized placement of control force: normalized positions on the x-axis (a) and y-axis (b).

Parts a and b of **Figure 3** show the geometric distribution of the control force x and y positions, respectively. Position was normalized by dividing distance along each axis by the corresponding plate dimension. The control force position shows a slight bias towards the upper right corner of the plate. As the disturbance force was consistently located at the antinode nearest the lower left corner of the plate, this indicates an effective repulsion between control and disturbance forces.

As with sensor position, a component-amplitude normalization was also undertaken for the control force location. Results are shown in **Figure 4**. A very slight preference exists towards locations with higher velocities. A stronger trend toward locations with low cross-derivative is apparent from the histogram on the right. Physically, a location with high cross-derivative is located between regions with out-of-phase displacements, which would impede good coupling between the control force and structure.

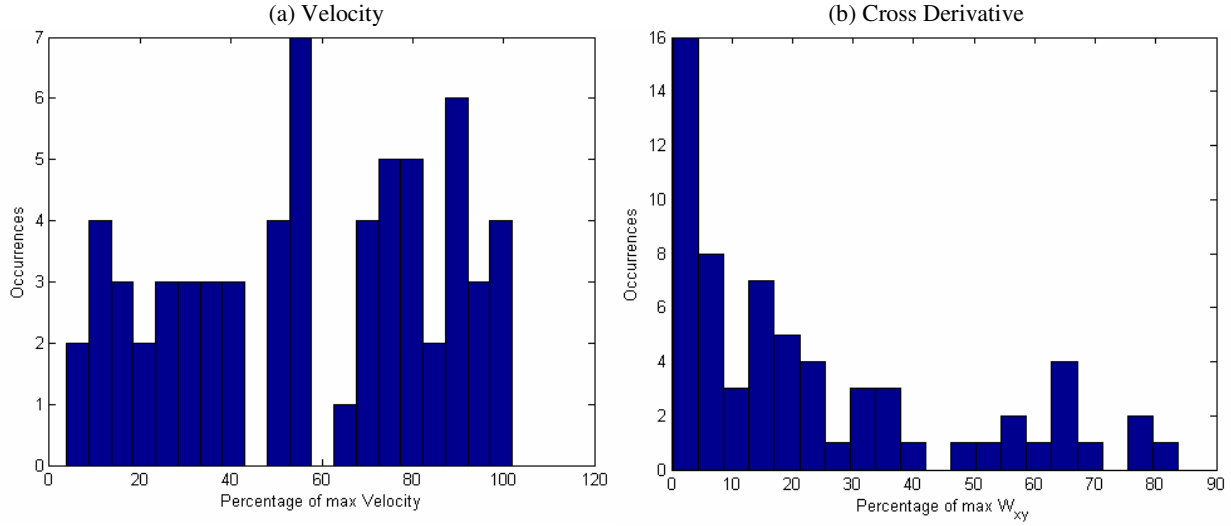

FIGURE 4. Sensor position distribution as a function of percentage of (a) velocity and (b) cross derivative level at forcing location compared to estimate of global maximum value.

The preceding results seem to indicate that in many respects, structural energy density control is comparable in implementation to velocity control. To determine if SED offers any benefit over simple velocity control, a simulation was performed in which the simply supported plate model used in the genetic algorithm was coupled with a modal radiation model for a rectangular enclosure. For this simulation, the SED sensor was placed at the center of the plate, that being the location corresponding to the antinodes of the most efficiently radiating structural modes (odd-odd). Disturbance and control forces were placed in opposite corners of the plate, 20% of the plate lengths away from the edges. Three types of control were simulated.

Figure 5 shows the control performance achieved for the three control scenarios. In each case, the dotted curve represents an estimate of the global acoustic potential energy in the enclosure in an uncontrolled state. The solid curve represents an estimate of the global acoustic potential energy after the application of a specific type of active control. Note that the frequency distribution is not uniform, but is primarily concentrated below 100 Hz.

The topmost portion (a) shows the attenuation achieved using acoustic potential energy control. While this type of control is not achievable in practice, it can be done in simulation and provides an estimate of the maximum achievable control using any method. A peak reduction of 67dB was achieved at the fundamental structural mode.

The middle portion (b) shows the attenuation of global potential energy achieved by controlling structural velocity at the sensor location. As can be seen, peak attenuation of 57 dB is achieved, but unwanted amplifications of up to 20 dB are present.

The bottommost portion (c) shows attenuation achieved upon minimization of the structural energy density at the sensor location. Although the peak attenuation of 57 dB is identical to that achieved using velocity control, structural energy density does show some advantage in that unwanted amplifications are not as severe at any frequency.

The plots shown are a single selection from a larger set of simulations. In some cases, depending on the configuration of sensors, forces, and location of the plate within the enclosure, none of the three methods provided good control. As a general rule, however, structural energy density control consistently caused less unwanted amplification than simple velocity control.

(a) Potential Energy Control

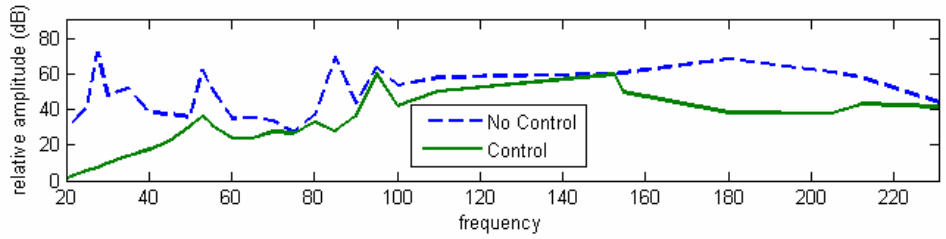

(b) Velocity Control

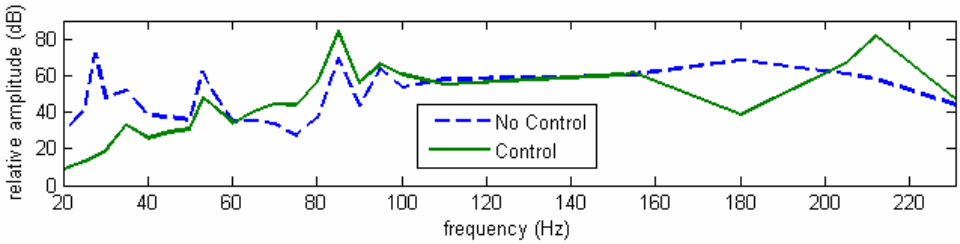

(c) Structural Energy Density Control

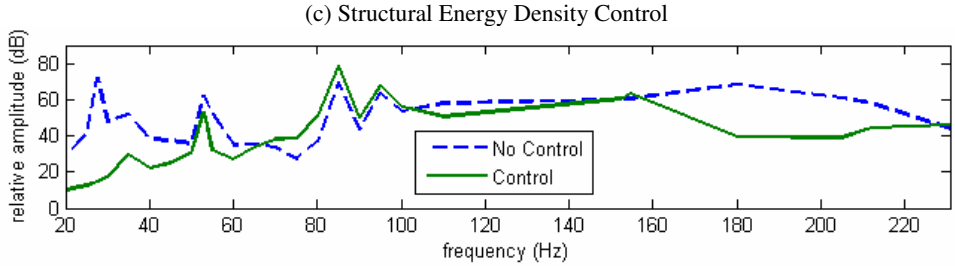

FIGURE 5. Potential energy reduction under potential energy control (a), velocity control (b), and structural energy density control (c)

Structural Energy Density Controllability

Structural energy density control does not suffer from the uncontrollabilities of two-dimensional power flow. The terms in structural energy density are mostly amplitude based, eliminating the problematic phase sensitivity of power flow. Additionally, the derivative terms are of a lower order, leaving them more connected with gross features of the structural response. Finally, the contours of structural energy density amplitude produced by varying control gain are nearly circular at all frequencies, leading to unique optima and ease of control system convergence. As a downside of implementing structural energy density control, 5, 7, or 9 accelerometers are required, depending on the interpolation scheme used. This is still superior to general power flow, which requires 13 accelerometers for a full 2-D near and far field measurement, although this can be reduced to 4 accelerometers in cases where certain assumptions about boundaries are sufficiently accurate.

CONCLUSIONS

Power flow and structural energy density were analyzed to determine if they could provide some of the same benefits to active structural acoustic control as energy based acoustic metrics do in active noise control. Power flow was found to be unsuitable for general use in an ASAC system due to lack of a unique minimum at many frequencies, and the strong effect of the sensor mass loading on the power flow field of a lightweight structure. Structural energy density was found to have good minimization behavior. A genetic algorithm was used to study placement of an SED sensor, and the optimal location at modal frequencies was found to coincide with antinodes, or regions of high velocity and low cross derivative. The placement of the control force is less critical, but in general coincides with regions of low cross derivative as well as general remoteness from the disturbance force. In the application of ASAC within an enclosure, SED-based control provides similar noise reduction to velocity control, and causes less undesired amplification.

ACKNOWLEDGMENTS

This work supported by NSF grant 0826554.

REFERENCES

1. S.D. Sommerfeldt and P.J. Nashif, *J. Acoust. Soc. Am.* **96**, 300-306 (1994).
2. D. U. Noiseaux, *J. Acoust. Soc. Am.* **47**, 238-247 (1970).
3. A. E. Schwenk, S. D. Sommerfeldt and S. I. Hayek, *J. Acoust. Soc. Am.* **95**, 2826-2835 (1994).
4. N. Tanaka, *Noise Control Engineering Journal* **44**, 23-33 (1996).
5. J. B. Piaud, *J. Acoust. Soc. Am.* **80**, 1114-1121 (1986).
6. J. Mei, *SPIE* **2717,** 399-403 (1996).
7. S. Timoshenko and D. Young, *Vibration Problems in Engineering*, New York: D. Van Norstrand Co., Inc, 1955, pp. 442.
8. A. Sakano and N. Tanaka, *JSME International Journal, Series C* **46**, 867-872 (2003).